

## Multidisciplinary study on the hydrogelation of digold(I) complex [{Au(<sup>9</sup>N-adeninate)}<sub>2</sub>(μ-dmpe)]: optical, rheological, and quasi-elastic neutron scattering perspectives

Daniel Blasco,<sup>a</sup> José M. López-de-Luzuriaga,<sup>\*a</sup> Miguel Monge,<sup>a</sup> M. Elena Olmos,<sup>a</sup> María Rodríguez-Castillo,<sup>a</sup> Hippolyte Amaveda,<sup>b</sup> Mario Mora,<sup>b</sup> Victoria García Sakai<sup>c</sup> and José A. Martínez-González.<sup>c</sup>

<sup>a</sup> Departamento de Química, Centro de Investigación en Síntesis Química (CISQ), Universidad de La Rioja, Madre de Dios 53, 26004 Logroño (Spain).

<sup>b</sup> Instituto de Nanociencia y Materiales de Aragón, INMA (CSIC-Universidad de Zaragoza), María de Luna 3, 50018 Zaragoza (Spain).

<sup>c</sup> ISIS Neutron and Muon Source, Rutherford Appleton Laboratory (RAL), Harwell Science and Innovation Campus, OX11 0QX Chilton, Didcot (United Kingdom).

### Electronic Supplementary Information

#### Table of Contents

1. Instrumentation .....	2
2. Syntheses of complexes <b>1-2</b> .....	5
3. Spectroscopic characterization of complexes <b>1-2</b> .....	6
3.1.    UATR-FTIR spectra .....	6
3.2.    FTIR spectra (nujol mulls) .....	7
3.3. <sup>1</sup> H and <sup>31</sup> P{ <sup>1</sup> H} NMR spectra of [(AuCl) <sub>2</sub> (μ-dmpe)] ( <b>1</b> ) .....	8
3.4. <sup>1</sup> H and <sup>31</sup> P{ <sup>1</sup> H} NMR spectra of [{Au( <sup>9</sup> N-adeninate)} <sub>2</sub> (μ-dmpe)] ( <b>2</b> ) ..	9
3.5.    ESI-MS spectra (for [{Au( <sup>9</sup> N-adeninate)} <sub>2</sub> (μ-dmpe)] ( <b>2</b> )) .....	10
4. Structural characterization of complex <b>2</b> .....	11
5. Optical properties .....	14
5.1.    Vis-UV spectra (H <sub>2</sub> O solution).....	14
5.2.    DRUV-Vis spectra (KBr mulls) .....	14
5.3.    Lifetime decay parameters of complex <b>2</b> .....	15
6. Computational studies.....	16
7. Hydrometallogel luminescence at different temperatures .....	18
8. Atomic coordinates of computational optimizations (xyz format) .....	19

## 1. Instrumentation.

**General procedures.**  $[\text{AuCl}(\text{tth})]$ ,<sup>1</sup>  $\text{Na}(\text{adeninate})$ ,<sup>2</sup> and  $[\text{Au}({}^9\text{N-adeninate})(\text{PMe}_3)]$ <sup>3</sup> were prepared according to previously published methods. Adenine (6-aminopurine) and 1,2-bis(dimethylphosphino)ethane (dmpe) were purchased from Merck and used as received. HPLC grade tetrahydrofuran (THF) was dried and degasified with a MBRAUN MB-SPS800 system prior to use. Distilled water was purged with nitrogen for 10 min prior to use for photophysical measurements in solution.

**Physical measurements.**  $^1\text{H}$  ( $\delta(\text{SiMe}_4) = 0.0$  ppm) and  $^{31}\text{P}\{{}^1\text{H}\}$  ( $\delta(85\% \text{ H}_3\text{PO}_4) = 0.0$  ppm) NMR spectra were recorded at 298 K with a Bruker ARX 300 spectrometer. UATR-IR spectra were recorded in the 4000-400  $\text{cm}^{-1}$  range with a Perkin-Elmer Two spectrophotometer equipped with a diamond crystal-UATR accessory. For the observing of  $\nu(\text{Au}-\text{Cl})$  stretching vibrations, FT-IR spectra were recorded in the 4000-200  $\text{cm}^{-1}$  range with a Perkin-Elmer FT-IR Spectrum 1000 spectrophotometer, using nujol mulls between polyethylene sheets. ESI-MS spectra were obtained with a Bruker MicroTOF-Q spectrometer with ESI ionisation source. CHNS elemental analysis were carried out with a Perkin-Elmer 240C microanalyser. UV-Vis absorption measurements were registered with a Hewlett-Packard 8453 diode array spectrophotometer in quartz cells (optical path = 1 cm). Diffuse reflectance UV-Vis spectra of pressed powder samples diluted with KBr were recorded on a Shimadzu UV-3600 spectrophotometer with a Harrick Praying Mantis accessory, and recalculated following the Kubelka-Munk function. Steady-state luminescence measurements were carried out in a Jobin-Yvon Horiba Fluorolog 3-22 Tau-3 spectrofluorimeter. Lifetime measurements were recorded with a Datastation HUB-B with a nanoLED controller and the DAS6 software. The nanoLED employed for lifetime measurements was one of 370 nm. Lifetime data were fitted with the Jobin-Yvon software package. The absolute photoluminescence quantum yield was determined with a Hamamatsu Quantaurus-QY C11347-11 spectrometer from a solid sample.

**Microscopy.** For a direct observation of liquid samples in its original state, specimens were vitrified in liquid ethane and analysed in a STEM microscope at low temperature. The vitrification method is a very fast sample cooling that prevents the formation of crystalline ice. Moreover, the thin layer of amorphous ice formed during the vitrification process protects the material from electron beam damage. The vitrification process was performed in a FEI Vitrobot: a 3  $\mu\text{L}$

---

<sup>1</sup> R. Usón, A. Laguna, M. Laguna, D. A. Briggs, H. H. Murray and J. P. Fackler, Jr., *(Tetrahydrothiophene)Gold(I) or Gold(III) Complexes in Inorganic Syntheses*, ed. H. D. Kaesz, Wiley-Interscience, 1989, **26**, pp. 85-91.

<sup>2</sup> H. Kawakami, H. Matsushita, Y. Naoi, K. Itoh and H. Yoshikoshi, *Chem. Lett.*, 1989, **18**, 235-238.

<sup>3</sup> D. Blasco, J. M. López-de-Luzuriaga, M. Monge, M. E. Olmos, D. Pascual and M. Rodríguez-Castillo, *Inorg. Chem.*, 2018, **57**, 3805-3817.

drop of an aqueous suspension of the material was placed on a TEM quantifoil carbon grid, the excess of water was blotted away at the Vitrobot with filter paper, and finally the grid was freeze-plunged in liquid ethane. Samples were then transferred under liquid nitrogen atmosphere to a Gatan TEM cryo-holder equipped with a liquid nitrogen reservoir. That way samples were handled and observed at T = 100 K. STEM images were obtained in a Tecnai F30 (FEI) operated at 300 kV and coupled with a High Angle Annular Dark Field (HAADF) detector.

**Crystallography.** Suitable single crystals were mounted in inert oil on MiteGen Micro Mounts and transferred to the cold nitrogen stream of either a Nonius Kappa CCD (**2**·1.25EtOH) or a Bruker APEX-II CCD (**2**·2H<sub>2</sub>O) area-detector diffractometer, both equipped with an Oxford Instruments low-temperature controller system (Mo K $\alpha$  = 0.71073 Å, graphite monochromator). Data was collected in  $\omega$  and  $\phi$  scan mode. Absorption corrections: semiempirical (based on multiple scans). The structure was solved by using direct methods and refined on  $F^2$  with SHELXL.<sup>4</sup> All non-hydrogen atoms were treated anisotropically, and all hydrogen atoms were included as riding bodies. CCDC 2080183-2080184 contain the supplementary crystallographic data for this paper. These data can be obtained free of charge via [www.ccdc.cam.ac.uk/data\\_request/cif](http://www.ccdc.cam.ac.uk/data_request/cif), or by emailing [data\\_request@ccdc.cam.ac.uk](mailto:data_request@ccdc.cam.ac.uk), or by contacting The Cambridge Crystallographic Data Center, 12 Union Road, Cambridge CB2 1EZ, UK; fax: +44 1223 336033.

**Rheology.** Rheological measurements were carried out in a HAAKE RheoStress 1 rheometer with a cone-plate system (Ti; diameter, 35 mm; cone angle, 1°), at a constant temperature of 25.0 ± 0.1 °C controlled with a cyclic water bath.

**Quasi-elastic neutron scattering experiments.** QENS experiments were performed on the near backscattering time-of-flight spectrometer IRIS at the ISIS Neutron and Muon Source (Didcot, United Kingdom).<sup>5</sup> IRIS was operated in the 002 pyrolytic graphite configuration (analysing energy of 1.84 meV) with a dynamic range from -0.4 to +0.4 meV, and a resolution (FWHM) of 17.5 μeV. The covered  $Q$  range was 0.42-1.85 Å<sup>-1</sup>.

Complexes [{Au(<sup>9</sup>N-adeninate)}<sub>2</sub>(μ-dmpe)] (**2**) and [Au(<sup>9</sup>N-adeninate)(PMe<sub>3</sub>)] (**3**) were dissolved in distilled water at a concentration of 10% (w/w), and transferred while fluid into PTFE-coated aluminium cans of annular geometry ( $\tau$  = 0.10 mm). Each sample was exposed to a total neutronic current of 600 μA at a controlled temperature of 284 K.

---

<sup>4</sup> G. M. Sheldrick, *SHELXL-97, Program for Crystal Structure Refinement*; University of Göttingen: Göttingen, Germany, 1997.

<sup>5</sup> ISIS Neutron and Muon Source, IRIS homepage: <https://www.isis.stfc.ac.uk/Pages/iris.aspx>.

**Computational details.** Theoretical calculations were performed with the Gaussian 09 package program.<sup>6</sup> Model systems  $\{[\text{Au}({}^9\text{N-adeninate})]_2(\mu\text{-dmpe})\}$  and  $\{[\text{Au}({}^9\text{N-adeninate})]_2(\mu\text{-dmpe})\}_2$  (**2a**) were built from the X-ray structure of **2**·EtOH, and were completely optimized at the DFT/PBE1PBE level of theory<sup>7</sup> with the third dispersion correction by Grimme (DFT-D3).<sup>8</sup> The following basis set combinations were employed: for gold, the quasi-relativistical (QR) 19-valence electrons (VE) pseudopotential (PP) from Andrae<sup>9</sup> and the corresponding basis sets augmented with two *f* polarisation functions were used.<sup>10</sup> Carbon, nitrogen, oxygen, fluorine, and phosphorus were treated by Stuttgart pseudopotentials,<sup>11</sup> including only the VE for each atom. For these atoms, the double- $\zeta$  basis set were used,<sup>12</sup> augmented by *d*-type polarisation functions.<sup>13</sup> For hydrogen, a double- $\zeta$  plus a *p*-type polarisation function was used.<sup>11</sup>

---

<sup>6</sup> Gaussian 09, Revision D.01, M.J. Frisch, G.W. Trucks, H.B. Schlegel, G.E. Scuseria, M.A. Robb, J.R. Cheeseman, G. Scalmani, V. Barone, B. Mennucci, G.A. Petersson, H. Nakatsuji, M. Caricato, X. Li, H.P. Hratchian, A.F. Izmaylov, J. Bloino, G. Zheng, J.L. Sonnenberg, M. Hada, M. Ehara, K. Toyota, R. Fukuda, J. Hasegawa, M. Ishida, T. Nakajima, Y. Honda, O. Kitao, H. Nakai, T. Vreven, J.A. Montgomery, Jr., J.E. Peralta, F. Ogliaro, M. Bearpark, J.J. Heyd, E. Brothers, K.N. Kudin, V.N. Staroverov, R. Kobayashi, J. Normand, K. Raghavachari, A. Rendell, J.C. Burant, S.S. Iyengar, J. Tomasi, M. Cossi, N. Rega, J.M. Millam, M. Klene, J.E. Knox, J.B. Cross, V. Bakken, C. Adamo, J. Jaramillo, R. Gomperts, R.E. Stratmann, O. Yazyev, A.J. Austin, R. Cammi, C. Pomelli, J.W. Ochterski, R.L. Martin, K. Morokuma, V.G. Zakrzewski, G.A. Voth, P. Salvador, J.J. Dannenberg, S. Dapprich, A.D. Daniels, Ö. Farkas, J.B. Foresman, J.V. Ortiz, J. Cioslowski, and D.J. Fox, Gaussian, Inc., Wallingford CT, 2009.

<sup>7</sup> J. P. Perdew, K. Burke and M. Ernzerhof, *Phys. Rev. Lett.*, 1996, **77**, 3865–3868.

<sup>8</sup> S. Grimme, *Wiley Interdiscip. Rev. Comput. Mol. Sci.*, 2011, **1**, 211-228.

<sup>9</sup> D. Andrae, U. Häussermann, M. Dolg, H. Stoll and H. Preuss, *Theor. Chim. Acta*, 1990, **77**, 123-141.

<sup>10</sup> P. Pyykkö, N. Runeberg and F. Mendizabal, *Chem. Eur. J.*, 1997, **3**, 1451-1457.

<sup>11</sup> A. Bergner, M. Dolg, W. Küchle, H. Stoll and H. Preuss, *Mol. Phys.*, 1993, **80**, 1431-1441.

<sup>12</sup> S. Huzinaga, in *Gaussian Basis Sets for Molecular Orbital Calculations*, Elsevier, 1984, p. 16.

<sup>13</sup> S. Huzinaga, *J. Chem. Phys.*, 1965, **42**, 1293-1302.

## 2. Syntheses of complexes **1-2**.

*Synthesis of [(AuCl)<sub>2</sub>(μ-dmpe)] (**1**)*. A well-stirred solution of [AuCl(tht)] (0.2500 g, 0.78 mmol) in 30 mL of anhydrous tetrahydrofuran, under nitrogen atmosphere, is prepared. Then, an appropriate volume of pure dmpe (0.39 mmol, 0.5:1 molar ratio with respect to [AuCl(tht)]) is added, causing the immediate formation of the desired product as a white solid. The mixture is kept under stirring for 2 h to ensure complete precipitation of [(AuCl)<sub>2</sub>(μ-dmpe)] (0.2323 g, 0.38 mmol), which is retrieved by filtration, and washed with 3 · 10 mL tetrahydrofuran + 1 · 10 mL *n*-hexane. Yield: 97%. <sup>1</sup>H NMR (300 MHz, *d*<sup>6</sup>-dmso): 2.19 (4H, ps, P(CH<sub>2</sub>)), 1.70-1.66 (12H, m, P(CH<sub>3</sub>)<sub>2</sub>). <sup>31</sup>P{<sup>1</sup>H} NMR (121 MHz, *d*<sup>6</sup>-dmso): 5.49 (s, [(CH<sub>3</sub>)<sub>2</sub>P(CH<sub>2</sub>)]<sub>2</sub>). FTIR (cm<sup>-1</sup>): 310 (AuCl). Anal. Calcd. for C<sub>6</sub>H<sub>16</sub>Au<sub>2</sub>Cl<sub>2</sub>P<sub>2</sub>: C, 11.72; H, 2.62. Found: C, 11.74; H, 2.64.

*Synthesis of [{Au(<sup>9</sup>N-adeninate)}<sub>2</sub>(μ-dmpe)] (**2**)*. Na(adeninate) (0.0395 g, 0.25 mmol) is added to a suspension of [(AuCl)<sub>2</sub>(μ-dmpe)] (0.0768 g, 0.13 mmol) in 20 mL of absolute ethanol. The mixture is stirred and refluxed for 2 h, leading to the disappearance of the gold(I) precursor and the precipitation of NaCl. After that time, the reaction flask is cooled to room temperature, and its contents filtered over Celite. The transparent filtrate is rotary evaporated up to a volume of *ca.* 2 mL, and 20 mL of *n*-hexane are added, leading to the precipitation of [{Au(<sup>9</sup>N-adeninate)}<sub>2</sub>(μ-dmpe)] (0.0838 g, 0.10 mmol) as a white solid. Yield: 82%. <sup>1</sup>H NMR (300 MHz, CD<sub>3</sub>OD): 8.13 (2H, s, <sup>2</sup>CH), 7.75 (2H, s, <sup>8</sup>CH), 2.43-2.40 (4H, AA'BB'XX' m, P(CH<sub>2</sub>)), 1.84-1.80 (12H, d, <sup>2</sup>J<sub>PH</sub> = 12 Hz, P(CH<sub>3</sub>)<sub>2</sub>). <sup>31</sup>P{<sup>1</sup>H} NMR (121 MHz, CD<sub>3</sub>OD): -1.21 (s, [(CH<sub>3</sub>)<sub>2</sub>P(CH<sub>2</sub>)]<sub>2</sub>). UATR-IR (cm<sup>-1</sup>): 3320 (NH), 3170 (NH). ESI-MS(+) (*m/z*): 678.1 ([Au<sub>2</sub>(μ-adeninate)(μ-dmpe)]<sup>+</sup>, calcd: 678.1). ESI-MS(-) (*m/z*): 134.0 ([adeninate]<sup>-</sup>, calcd. 134.0). Anal. Calcd. for C<sub>16</sub>H<sub>24</sub>Au<sub>2</sub>N<sub>10</sub>P<sub>2</sub>: C, 23.66; H, 2.98; N, 17.24. Found: C, 23.63; H, 2.31; N, 17.22.

3. Spectroscopic characterization of complexes **1-2**.

3.1. UATR-FTIR spectra.

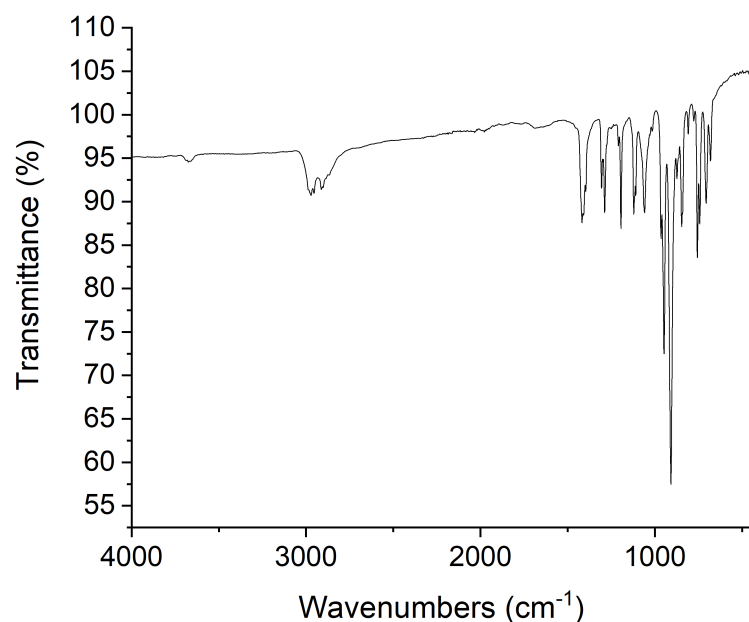


**Figure S1.** UATR-IR spectrum of  $[(\text{AuCl})_2(\mu\text{-dmpe})]$  (**1**).

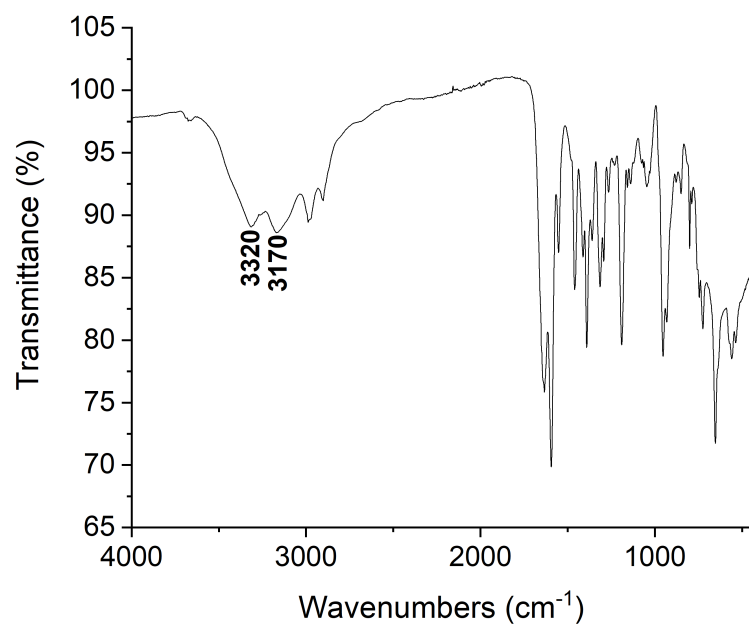


**Figure S2.** UATR-IR spectrum of  $\{[\text{Au}(^9\text{N-adeninate})_2](\mu\text{-dmpe})\}$  (**2**).

3.2. FTIR spectra (nujol mulls).

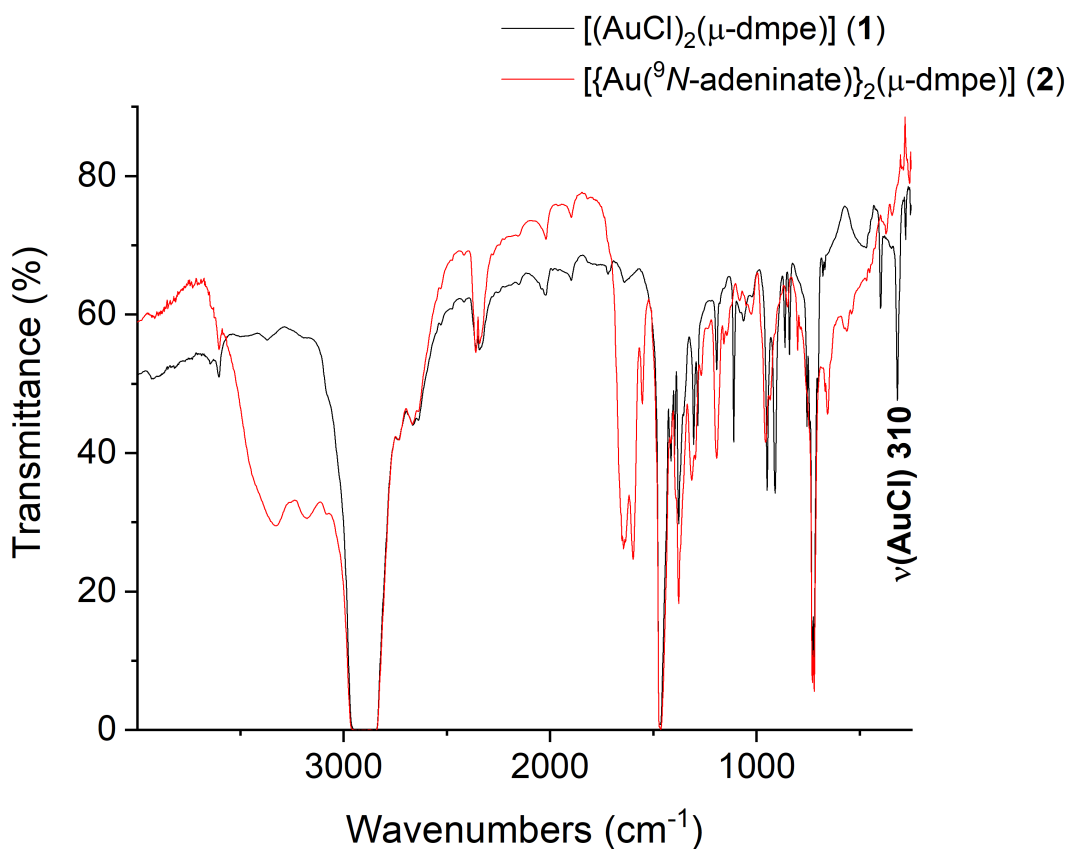


**Figure S3.** Superimposition of the FTIR spectra of  $[(\text{AuCl})_2(\mu\text{-dmpe})] (\mathbf{1}$ , black line) and  $\{[\text{Au}(^9\text{N-adeninate})]_2(\mu\text{-dmpe})\} (\mathbf{2}$ , red line).

3.3.  $^1\text{H}$  and  $^{31}\text{P}\{^1\text{H}\}$  NMR spectra of  $[(\text{AuCl})_2(\mu\text{-dmpe})]$  (**1**).

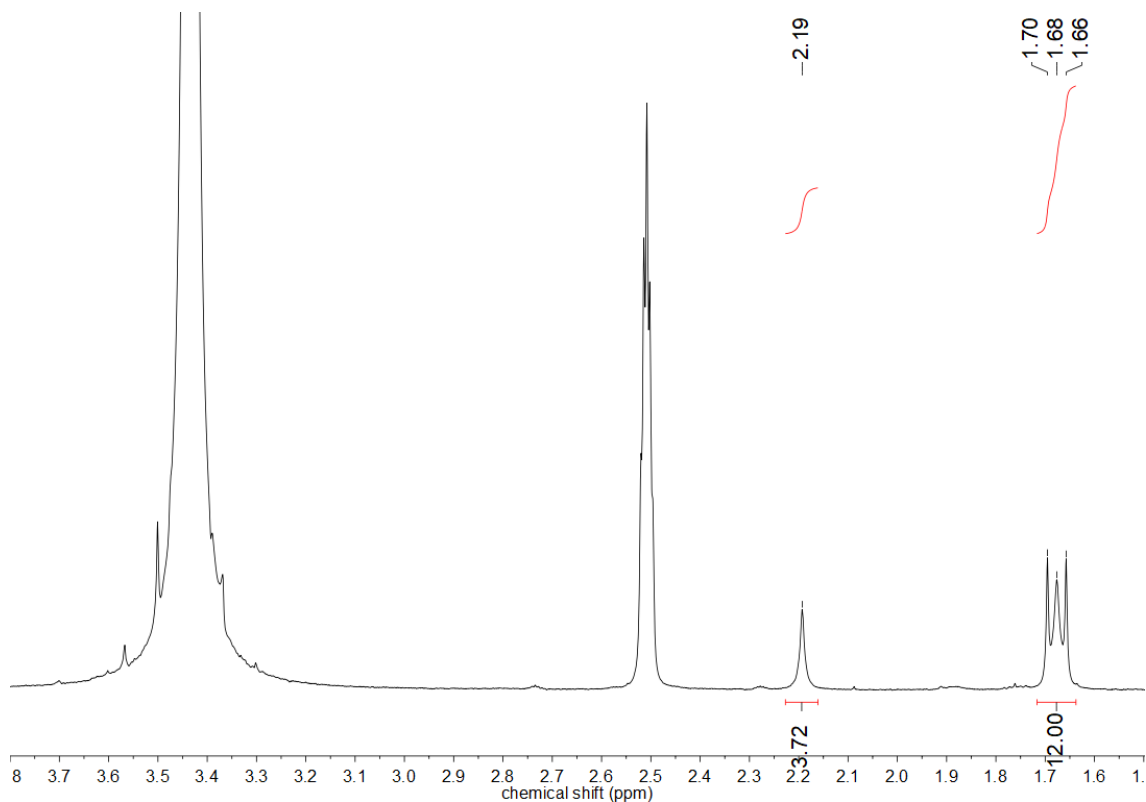


**Figure S4.**  $^1\text{H}$  NMR spectrum (300 MHz,  $(\text{CD}_3)_2\text{SO}$ ) of  $[(\text{AuCl})_2(\mu\text{-dmpe})]$  (**1**).

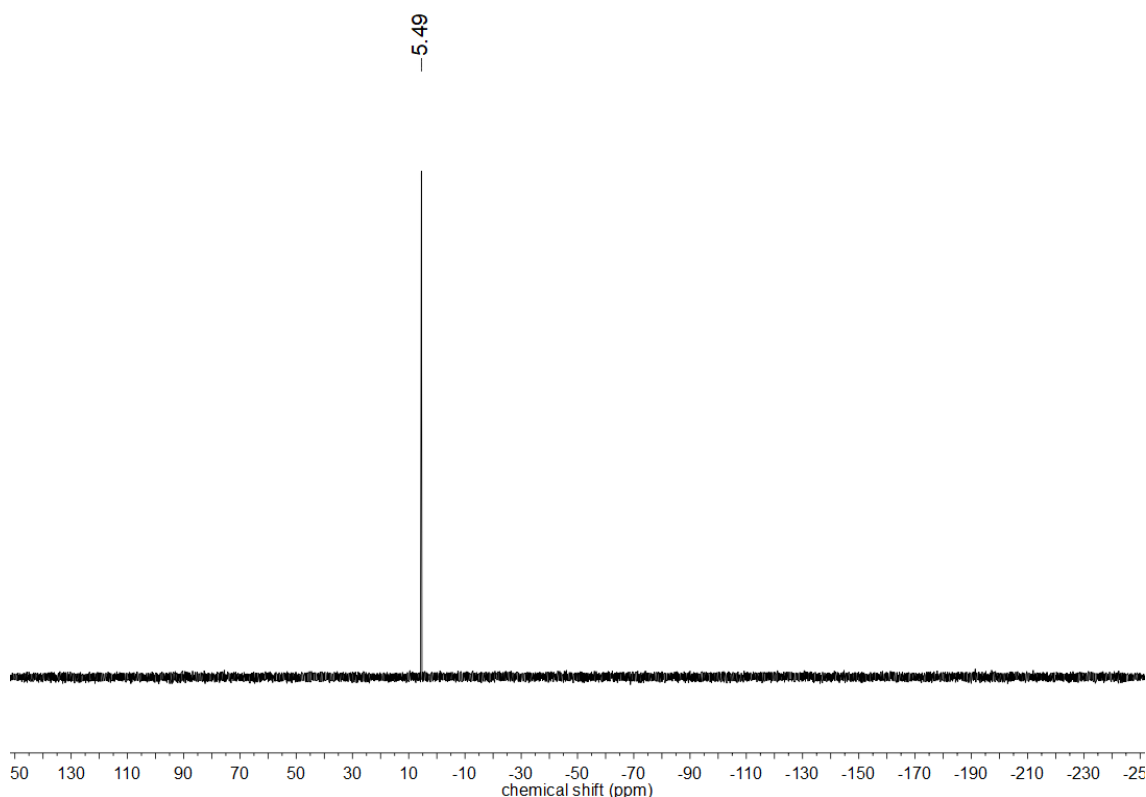


**Figure S5.**  $^{31}\text{P}\{^1\text{H}\}$  NMR spectrum (121 MHz,  $(\text{CD}_3)_2\text{SO}$ ) of  $[(\text{AuCl})_2(\mu\text{-dmpe})]$  (**1**).

3.4.  $^1\text{H}$  and  $^{31}\text{P}\{{}^1\text{H}\}$  NMR spectra of  $[\{\text{Au}(^9\text{N-adeninate})\}_2(\mu\text{-dmpe})]$  (**2**).

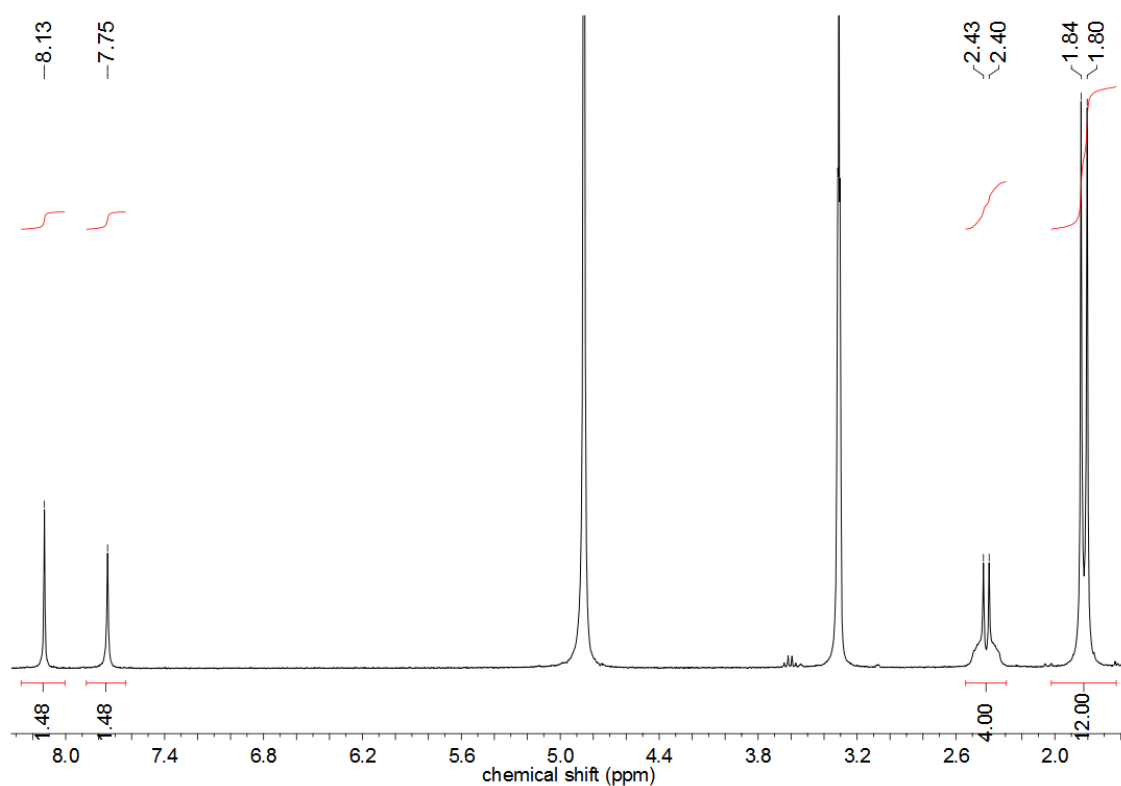


**Figure S6.**  $^1\text{H}$  NMR spectrum (300 MHz,  $\text{CD}_3\text{OD}$ ) of  $[\{\text{Au}(^9\text{N-adeninate})\}_2(\mu\text{-dmpe})]$  (**2**).

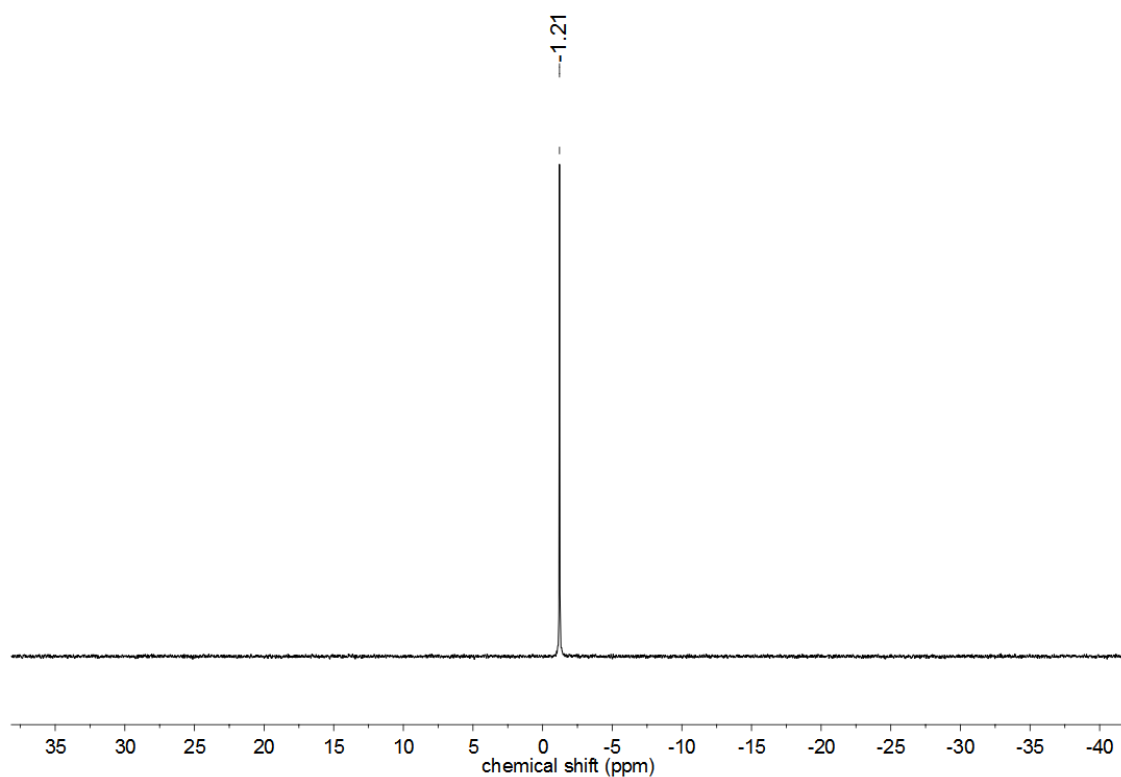


**Figure S7.**  $^{31}\text{P}\{{}^1\text{H}\}$  NMR spectrum (121 MHz,  $\text{CD}_3\text{OD}$ ) of  $[\{\text{Au}(^9\text{N-adeninate})\}_2(\mu\text{-dmpe})]$  (**2**).

3.5. ESI-MS spectra (for  $\{[\text{Au}({}^9\text{N-adeninate})]_2(\mu\text{-dmpe})\}$  (**2**)).

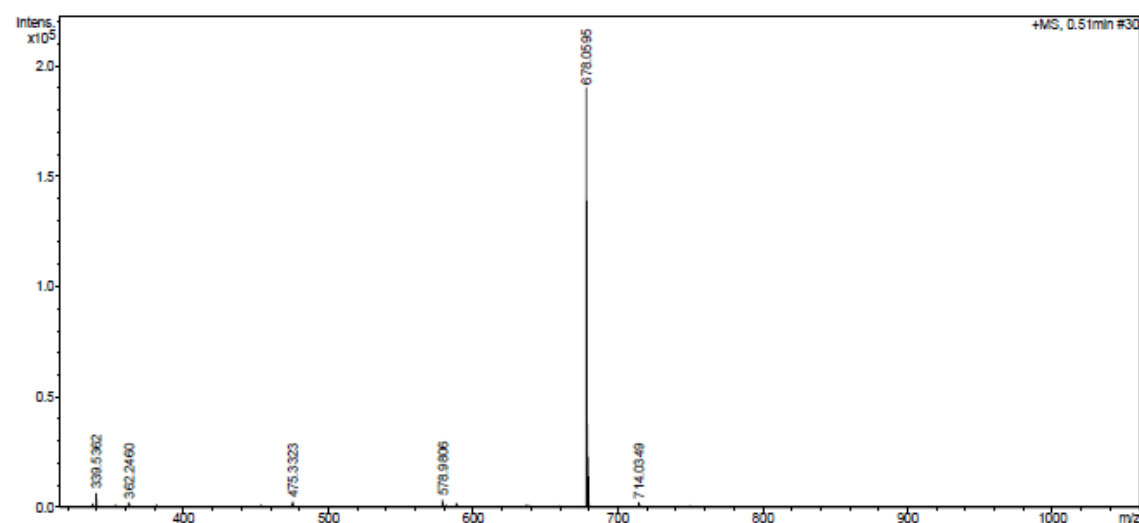


Figure S8. ESI-MS(+) spectrum of  $\{[\text{Au}({}^9\text{N-adeninate})]_2(\mu\text{-dmpe})\}$  (**2**).

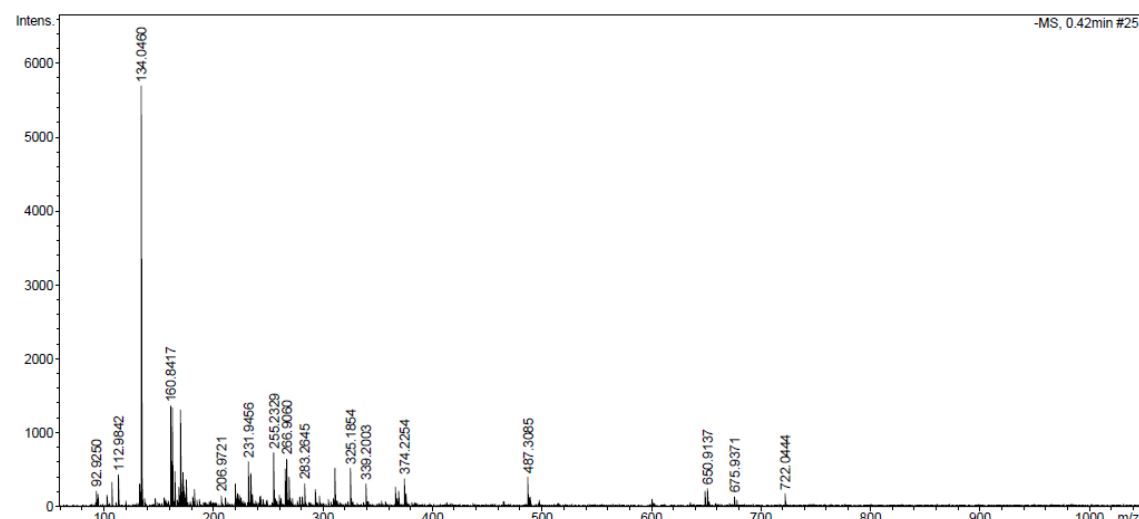


Figure S9. ESI-MS(-) spectrum of  $\{[\text{Au}({}^9\text{N-adeninate})]_2(\mu\text{-dmpe})\}$  (**2**).

#### 4. Structural characterization of complex **2**.

**Table S1.** Data collection and structure refinement details for **2·1.25EtOH** and **2·2H<sub>2</sub>O**.

Parameter	Value(s) (for <b>2·1.25EtOH</b> )		Value(s) (for <b>2·2H<sub>2</sub>O</b> )	
Diffractometer	Nonius Kappa CCD		Bruker APEX-II CCD	
Empirical formula	$C_{16}H_{24}Au_2N_{10}P_2\cdot1.25C_2H_6O$		$C_{16}H_{24}Au_2N_{10}P_2\cdot2H_2O$	
Formula mass	$869.91 \text{ g}\cdot\text{mol}^{-1}$		$848.36 \text{ g}\cdot\text{mol}^{-1}$	
Crystal habit	Colorless prism		Colorless needle	
Temperature	173(2) K		135 K	
Wavelength	0.71073 Å		0.71073 Å	
Crystal system	Triclinic		Triclinic	
Space group	<i>P</i> -1		<i>P</i> -1	
	<i>a</i> = 9.1501(6) Å	$\alpha$ = 99.383(3)°	<i>a</i> = 9.5407(7) Å	$\alpha$ = 101.704(2)°
Unit cell dimensions	<i>b</i> = 10.3807(7) Å	$\beta$ = 96.405(4)°	<i>b</i> = 11.8809(9) Å	$\beta$ = 108.921(2)°
	<i>c</i> = 17.7940(11) Å	$\gamma$ = 113.464(3)°	<i>c</i> = 13.2305(10) Å	$\gamma$ = 112.234(2)°
Volume	1500.29(17) Å <sup>3</sup>		1219.05(16) Å <sup>3</sup>	
<i>Z</i>	2		2	
Density (calculated)	1.900 Mg·m <sup>-3</sup>		2.311 Mg·m <sup>-3</sup>	
Absorption coefficient	9.903 mm <sup>-1</sup>		12.187 mm <sup>-1</sup>	
<i>F</i> (000)	821		796.0	
Crystal size	0.3 x 0.250 x 0.175 mm <sup>3</sup>		0.183 x 0.06 x 0.025 mm <sup>3</sup>	
$\vartheta$ range ( $2\vartheta_{\max}/\vartheta$ )	55 -11 $\leftarrow$ <i>h</i> $\leftarrow$ 11		54 -12 $\leftarrow$ <i>h</i> $\leftarrow$ 12	
Index ranges	-13 $\leftarrow$ <i>k</i> $\leftarrow$ 13 -23 $\leftarrow$ <i>l</i> $\leftarrow$ 22		-14 $\leftarrow$ <i>k</i> $\leftarrow$ 15 -16 $\leftarrow$ <i>l</i> $\leftarrow$ 16	
Total reflections	20031		24311	
Independent reflections	6790 [ $R_{\text{int}} = 0.0598$ ]		5389 [ $R_{\text{int}} = 0.0487$ ]	
Completeness to $\theta = 25.242^\circ$	99.6%		99.8%	
Refinement method	Full-matrix least-squares on $F^2$		Full-matrix least-squares on $F^2$	
Data / Restraints / Parameters	6790 / 12 / 325		5389 / 0 / 293	
Goodness-of-fit on $F^2$	1.142		1.060	
Final <i>R</i> indexes [ $ I  > 2\sigma(I)$ ]	$R_1 = 0.0708$ , $wR_2 = 0.1843$		$R_1 = 0.0291$ , $wR_2 = 0.0623$	
Final <i>R</i> indexes (all data)	$R_1 = 0.0856$ , $wR_2 = 0.1927$		$R_1 = 0.0418$ , $wR_2 = 0.0682$	
Largest diff. peak and hole (e/Å <sup>3</sup> )	2.95, -3.83		1.95, -1.85	

**Table S2.** Selected bond lengths ( $\text{\AA}$ ) and angles ( $^\circ$ ) for **2**·1.25EtOH.

Au1-N1	2.030(11)
Au2-N2	2.027(11)
Au1-P1	2.238(4)
Au2-P2	2.241(4)
Au1···Au2	2.9921(7)
N1-Au1-P1	175.0(4)
N2-Au2-P2	178.0(3)

**Table S3.** Selected hydrogen bond lengths ( $\text{\AA}$ ) and angles ( $^\circ$ ) for **2**·1.25EtOH.

D-H···A	d(D-H)	d(H···A)	d(D···A)	$\theta(\text{D-H}\cdots\text{A})$
C10-H1···Au2 <sup>#1</sup>	0.93	2.82	3.749(3)	176.0
N5-H5E···N2 <sup>#2</sup>	0.86	2.06	2.90(2)	163.6
N10-H10A···N9 <sup>#3</sup>	0.86	2.15	3.01(2)	172.2
O1-H1···N4 <sup>#4</sup>	0.82	2.34	2.79(2)	114.7
N10-H10B···O2 <sup>#5</sup>	0.86	2.09	2.94(5)	166.4

Symmetry transformations used to generate equivalent atoms:

#1:  $x, y - 1, z$ ; #2:  $-x + 2, -y + 1, -z + 1$ ; #3:  $-x + 2, -y + 2, -z + 1$ ; #4:  $x + 2, -y + 2, -z$ ; #5:  $x + 1, y + 1, z$ .**Table S4.** Selected bond lengths ( $\text{\AA}$ ) and angles ( $^\circ$ ) for **2**·2H<sub>2</sub>O.

Au1-N1	2.049(5)
Au2-N6	2.060(5)
Au1-P1	2.2436(15)
Au2-P2	2.2472(15)
Au1···Au2	3.0512(3)
N1-Au1-P1	177.63(14)
N6-Au2-P2	177.27(15)

**Table S5.** Selected hydrogen bond lengths ( $\text{\AA}$ ) and angles ( $^\circ$ ) for **2**·2H<sub>2</sub>O.

D-H···A	d(D-H)	d(H···A)	d(D···A)	$\theta(\text{D-H}\cdots\text{A})$
N5-H5A···N7 <sup>#1</sup>	0.88	2.320	3.125	151.97
N5-H5B···N2 <sup>#1</sup>	0.88	2.118	2.979	165.70
N10-H10A···N8 <sup>#2</sup>	0.88	2.205	3.034	156.80
N10-H10B···O1	0.88	2.148	2.970	155.21
O1-H1D···N3 <sup>#3</sup>	0.87	2.130	2.956	158.60
O1-H1E···N4 <sup>#1</sup>	0.87	2.015	2.866	165.73

Symmetry transformations used to generate equivalent atoms:

#1:  $-x + 2, -y + 2, -z + 1$ ; #2:  $-x + 1, -y + 2, -z$ ; #3:  $x, y + 1, z$ .

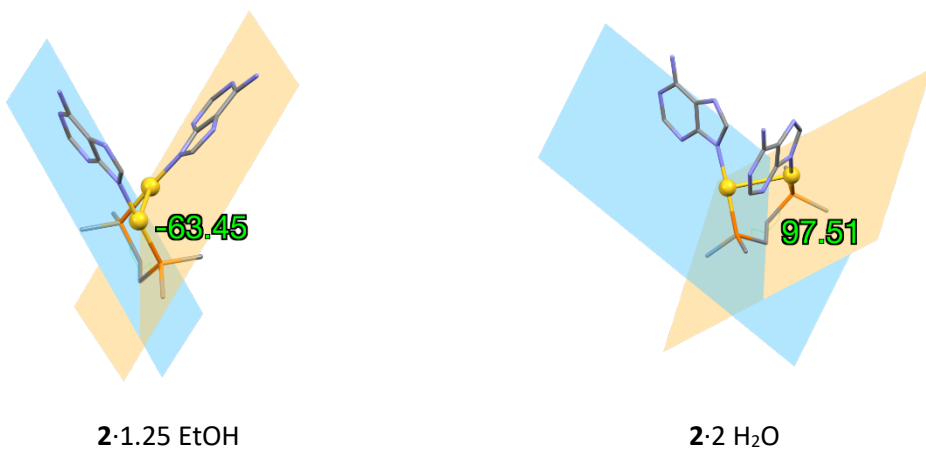


**Figure S10.** Views of the asymmetric unit of **2·1.25EtOH** (left) and **2·2H<sub>2</sub>O** (right) along the C-C bridge bond, where the P-C-C planes have been highlighted. Solvent molecules and hydrogen atoms have been omitted for clarity. Colour code: C, grey; Au, yellow; N, blue; P, orange.

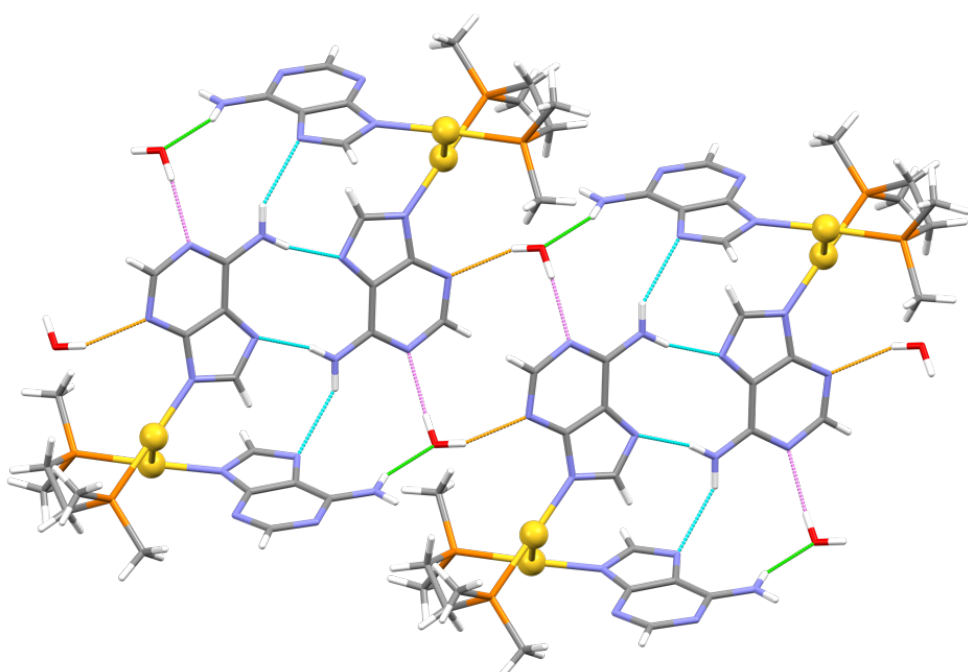


**Figure S11.** Fragment of the bidimensional expansion of **2·2H<sub>2</sub>O** including  $^6\text{CN}-\text{H}\cdots\text{N}$  (blue dashes),  $\text{O}-\text{H}\cdots\text{N}$  (violet dashes),  $\text{O}-\text{H}\cdots\text{N}$  (orange dashes) and  $^6\text{CN}-\text{H}\cdots\text{O}$  hydrogen bonds (green dashes). Colour code: C, grey; H, white; Au, yellow; N, blue; O, red; P, orange.

5. Optical properties.

5.1. Vis-UV spectra ( $\text{H}_2\text{O}$  solution).

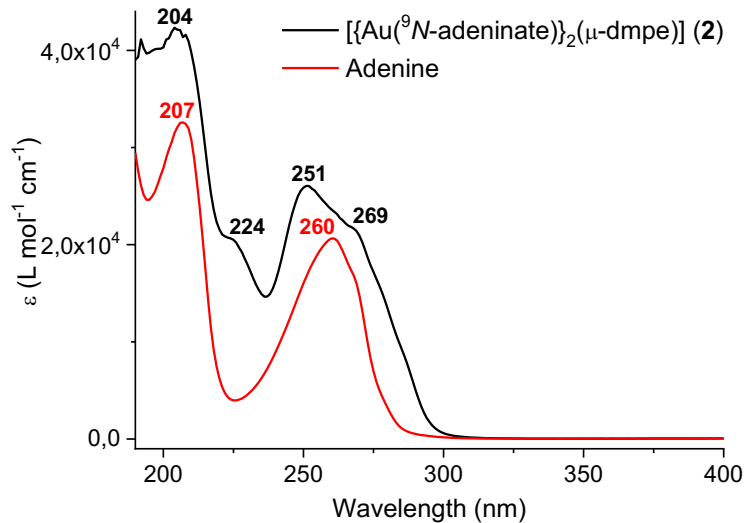


**Figure S12.** Superimposition of the absorption spectra of  $[\{\text{Au}^{9\text{N-adeninate}}\}_2(\mu\text{-dmpe})]\text{ (2)}$ , black line) and free adenine (red line) in aqueous solution.

5.2. DRUV-Vis spectra (KBr mulls).

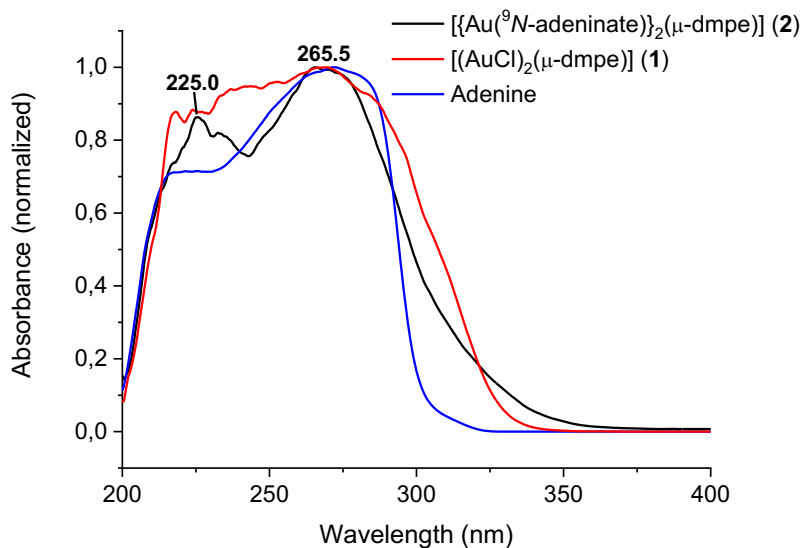


**Figure S13.** Superimposition of the absorption spectra of  $[\{\text{Au}^{9\text{N-adeninate}}\}_2(\mu\text{-dmpe})]\text{ (2)}$ , black line),  $[(\text{AuCl})_2(\mu\text{-dmpe})]\text{ (1)}$ , red line) and free adenine (blue line) in KBr mulls.

### 5.3. Lifetime decay parameters of complex 2.

Single Photon Counting data were fitted to the multiexponential decay function (**Equation 1**):

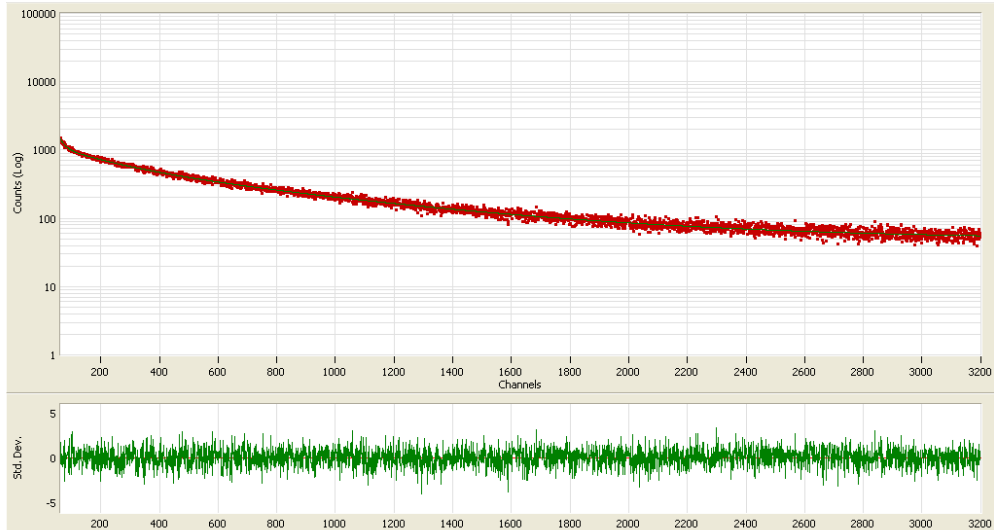
$$f(i) = A + \sum_n B_n \cdot \exp\left(-\frac{i}{T_n}\right) \quad \text{Equation 1}$$

where  $A$ ,  $B_n$  and  $T_n$  are free fitting parameters and  $n$  is a variable integer between 1 and 4.

Lifetime decay parameters for complex 2 at 298 K ( $n = 3$ ):

$n$	$T_n$ (channels)	$T_n$ (s)	$\sigma_n$ (s)	$B_n$	Rel. Ampl. (%)	$\sigma_n$
1	173.575	3.047681E-07	1.446541E-08	428.0221	15.13	5.337056
2	700.4806	1.229925E-06	9.995937E-09	585.2627	83.47	1.998551
3	18.01985	3.163979E-08	2.303366E-09	384.0366	1.41	14.00189

$A = 48.80651$ ;  $\chi^2 = 1.01105$  (3132 degrees of freedom);  $\tau = 617$  ns.



Lifetime decay parameters for complex 2 at 77 K ( $n = 1$ ):

$n$	$T_n$ (channels)	$T_n$ (s)	$\sigma_n$ (s)	$B_n$	Rel. Ampl. (%)	$\sigma_n$
1	397.9412	1.397434E-06	1.384673E-08	206.6542	100.00	1.166517

$A = 101.6438$ ;  $\chi^2 = 1.058434$  (3738 degrees of freedom);  $\tau = 1397$  ns.



6. Computational studies.

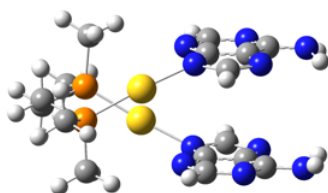


**Figure S14.** Structural result of the optimization of a  $\{[\text{Au}({}^9\text{N-adeninate})_2](\mu\text{-dmpe})\}$  single molecule, at the DFT-D3/PBE level of theory. A new  $\pi$ -stacking interaction, which is absent in the crystalline structure of **2·1.25EtOH**, is established.

**Table S6.** Selected bond lengths ( $\text{\AA}$ ), angles ( $^\circ$ ), and torsions ( $^\circ$ ) for **2·1.25EtOH** and model **2a**.

Bond lengths ( $\text{\AA}$ ), angles ( $^\circ$ ), and torsions ( $^\circ$ )	<b>2·1.25EtOH</b> (X-ray)	Model <b>2a</b>
Au-P	2.238(4)	2.27
	2.241(4)	2.28
Au-N	2.026(12)	2.03
	2.034(12)	2.04
Au <sup>I</sup> ...Au <sup>I</sup>	2.9919(8)	2.99
N-Au-P	175.0(4)	172.0
	178.1(4)	177.0
N-Au <sup>I</sup> ...Au <sup>I</sup> -N	62.76	68.8
P-C-C-P	63.43	58.9

**Table S7.** Most relevant TD-DFT singlet-to-singlet and singlet-to-triplet transitions of model **2a**.

Transition	Wavelength (nm)	Oscillator strength	Contributions (%)
B $S_0 \rightarrow S_{30}$	274.80	0.1395	$179 \rightarrow 187$ (39)
			$180 \rightarrow 188$ (40)
C $S_0 \rightarrow S_{56}$	246.34	0.1594	$185 \rightarrow 201$ (16)
			$186 \rightarrow 202$ (60)
D $S_0 \rightarrow S_{72}$	239.40	0.4532	$185 \rightarrow 201$ (17)
			$185 \rightarrow 204$ (19)
			$186 \rightarrow 203$ (32)
E $S_0 \rightarrow S_{84}$	236.76	0.1182	$183 \rightarrow 195$ (7)
			$184 \rightarrow 196$ (8)
			$186 \rightarrow 206$ (11)
F $S_0 \rightarrow S_{97}$	230.45	0.0975	$185 \rightarrow 205$ (14)
			$186 \rightarrow 215$ (24)
A $S_0 \rightarrow T_1$	379.41	Spin forbidden	$185 \rightarrow 188$ (26)
			$186 \rightarrow 187$ (51)

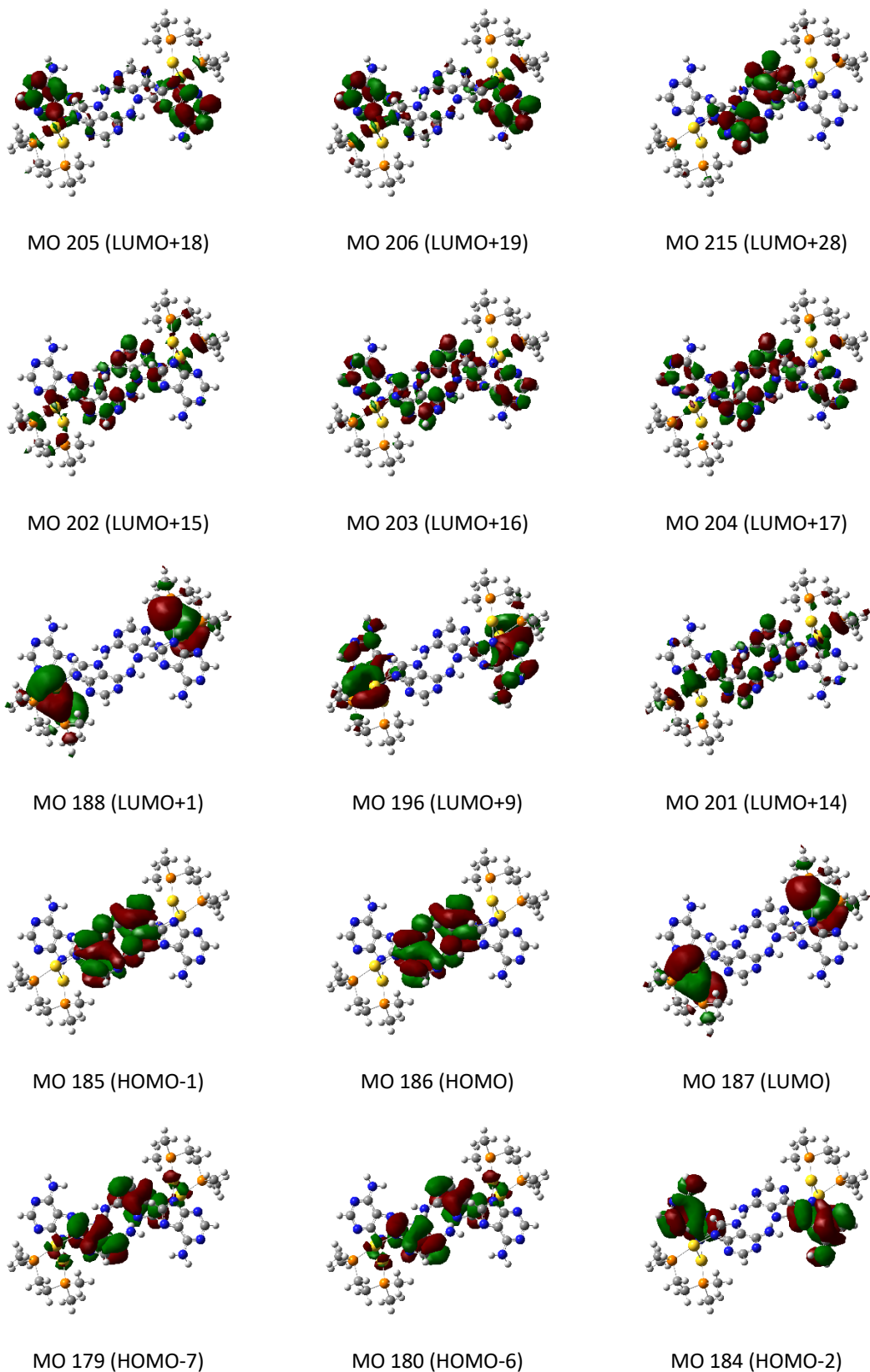


**Figure S15.** Selected molecular orbitals of model 2a.

7. Hydrometallogel luminescence at different temperatures.

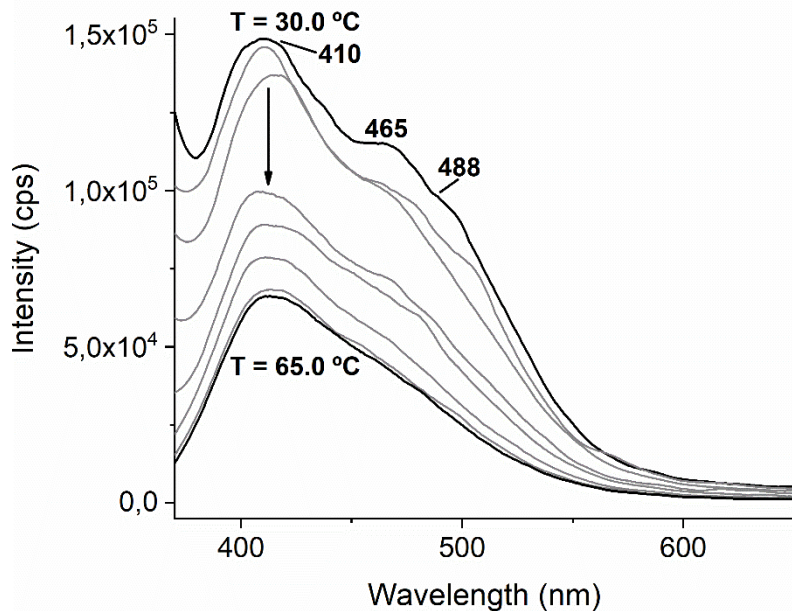


**Figure S16.** Emission spectra ( $\lambda_{\text{ex}} = 354 \text{ nm}$ ) of the hydrometallogel of  $[\{\text{Au}({}^9\text{N-adeninate})(\mu\text{-dmpe})\}]$  (**2**), at different temperatures in the  $30 \text{ }^\circ\text{C}$ - $60 \text{ }^\circ\text{C}$  range (collected each  $5 \text{ }^\circ\text{C}$  interval). The vertical arrow denotes the intensity drop associated with the gel-to-sol thermotropic transition.

7. Atomic coordinates of computational optimizations (xyz format).

**Table S8.** Atomic coordinates of the optimization of [{Au(<sup>9</sup>N-adeninate)}<sub>2</sub>(μ-dmpe)].

C	2.28461000	-1.07050400	1.89306500
C	2.95389400	0.89317600	1.59095100
C	1.55794400	0.93079000	1.54823600
C	3.62138000	2.08980200	1.29471700
C	1.57770800	3.09212300	1.06397000
C	1.55791600	-0.93080000	-1.54826200
C	2.95386700	-0.89319600	-1.59096400
C	2.28460000	1.07048800	-1.89309300
C	1.57765900	-3.09212900	-1.06398300
C	3.62134000	-2.08982300	-1.29470900
C	-4.08748900	-0.64450100	0.40360400
C	-4.08748800	0.64452600	-0.40355800
C	-2.51839700	-2.09528000	-1.59779000
C	-3.26499000	-3.34917800	0.91362500
C	-2.51835200	2.09529100	1.59781300
C	-3.26497500	3.34919500	-0.91359100
N	1.13001700	-0.34891800	1.75067300
N	1.12999900	0.34891200	-1.75070900
N	3.39940600	-0.38205100	1.81513900
N	2.90584500	3.18862100	1.03730100
N	0.82359400	2.02639400	1.29819800
N	3.39939000	0.38202700	-1.81515400
N	2.90579500	-3.18863500	-1.03729600
N	0.82355500	-2.02639600	-1.29822500
P	-2.62885700	-1.78000700	0.20147900
P	-2.62884300	1.78002000	-0.20145300
Au	-0.67534600	-1.04568400	1.09746300
Au	-0.67534900	1.04568900	-1.09747100
H	2.25041900	-2.14912600	2.04497900
H	1.03764400	4.02218500	0.85008500
H	2.25041800	2.14910900	-2.04501400
H	1.03758600	-4.02218600	-0.85009900
H	-4.15350900	-0.43170300	1.48153300
H	-4.98461200	-1.22861300	0.14042000
H	-4.98460100	1.22864800	-0.14036500
H	-4.15352100	0.43173000	-1.48148700
H	-2.32057100	-1.13949500	-2.10308800
H	-1.63470500	-2.72371700	-1.77052500
H	-3.43916600	-2.55897200	-1.97944600
H	-4.19123500	-3.66527800	0.41213700
H	-3.44680100	-3.21117200	1.98768100
H	-2.49433300	-4.12132200	0.78763600
H	-1.63462800	2.72368700	1.77053700
H	-3.43909600	2.55902200	1.97948000
H	-2.32056300	1.13949800	2.10311000
H	-2.49431100	4.12133400	-0.78761700
H	-4.19120900	3.66530600	-0.41208700
H	-3.44680700	3.21118900	-1.98764400
N	4.97007800	-2.16611500	-1.27172800
H	5.45627600	-1.28418200	-1.18003800
H	5.35571600	-2.95800200	-0.77479600
N	4.97011800	2.16608800	1.27176000
H	5.45631700	1.28415500	1.18007800
H	5.35577000	2.95798000	0.77484500

**Table S9.** Atomic coordinates of the optimization of model **2a**.

C	0.33736400	-1.19647600	-2.88859700
C	-1.42564100	-1.01992300	-1.73657200
C	-1.80686200	-1.43440400	-3.01198500
C	-2.45322600	-0.87953800	-0.77661100
C	-3.93197200	-1.50346200	-2.42959800
C	2.61380000	-0.03190400	-5.30488100
C	3.56793000	-0.18135500	-4.29517100
C	2.32820100	1.42020200	-3.73224300
C	3.42010100	-1.77988300	-6.39606400
C	4.47830900	-1.24002700	-4.43886300
C	-2.43121600	-0.46129700	-8.43867300
C	-2.46859300	1.03804200	-8.19342300
C	0.46126000	-0.40883000	-8.89529800
C	-1.01311600	-2.91013500	-8.97287400
C	-3.46611600	0.94798300	-5.42319900
C	-2.65617200	3.43889400	-6.66583500
N	-0.65929600	-1.55263200	-3.74681600
N	1.82165000	1.01743400	-4.93517000
N	-0.06053700	-0.87289700	-1.67953400
N	-3.71432500	-1.14396600	-1.16831900
N	-3.06358900	-1.66686000	-3.42097300
N	3.37224600	0.74527000	-3.30549400
N	4.37976000	-2.03608200	-5.50747100
N	2.50631200	-0.81912000	-6.38576300
P	-0.84784500	-1.34540500	-8.02634200
P	-2.16034700	1.67946800	-6.47399000
Au	-0.63947100	-1.55688900	-5.77754200
Au	-0.04063400	1.37318500	-5.69479000
C	-0.33736400	1.19647600	2.88859700
C	1.42564100	1.01992300	1.73657200
C	1.80686200	1.43440400	3.01198500
C	2.45322600	0.87953800	0.77661100
C	3.93197200	1.50346200	2.42959800
C	-2.61380000	0.03190400	5.30488100
C	-3.56793000	0.18135500	4.29517100
C	-2.32820100	-1.42020200	3.73224300
C	-3.42010100	1.77988300	6.39606400
C	-4.47830900	1.24002700	4.43886300
C	2.43121600	0.46129700	8.43867300
C	2.46859300	-1.03804200	8.19342300
C	-0.46126000	0.40883000	8.89529800
C	1.01311600	2.91013500	8.97287400
C	3.46611600	-0.94798300	5.42319900
C	2.65617200	-3.43889400	6.66583500
N	0.65929600	1.55263200	3.74681600
N	-1.82165000	-1.01743400	4.93517000
N	0.06053700	0.87289700	1.67953400
N	3.71432500	1.14396600	1.16831900
N	3.06358900	1.66686000	3.42097300
N	-3.37224600	-0.74527000	3.30549400
N	-4.37976000	2.03608200	5.50747100
N	-2.50631200	0.81912000	6.38576300
P	0.84784500	1.34540500	8.02634200
P	2.16034700	-1.67946800	6.47399000
Au	0.63947100	1.55688900	5.77754200
Au	0.04063400	-1.37318500	5.69479000

N	5.45491800	-1.46721400	-3.54098100
N	-2.21801700	-0.51714800	0.48016200
N	2.21801700	0.51714800	-0.48016200
N	-5.45491800	1.46721400	3.54098100
H	-0.09833000	-3.50033000	-8.82804200
H	-1.86207600	-3.48087300	-8.57355800
H	-1.16185000	-2.71208400	-10.04433100
H	1.86207600	3.48087300	8.57355800
H	0.09833000	3.50033000	8.82804200
H	1.16185000	2.71208400	10.04433100
H	1.42521600	-0.87201300	-8.65018900
H	0.27452600	-0.38384800	-9.97851100
H	0.49938600	0.60824400	-8.48109300
H	-0.27452600	0.38384800	9.97851100
H	-1.42521600	0.87201300	8.65018900
H	-0.49938600	-0.60824400	8.48109300
H	-3.21560700	-0.97445100	-7.86139000
H	-2.64227300	-0.64730300	-9.50464300
H	-1.73979100	1.55833700	-8.83407900
H	-3.46314800	1.42022200	-8.47691000
H	-1.97292100	3.93508300	-7.36795500
H	-3.69107500	3.51633500	-7.02979600
H	-2.57096600	3.93248200	-5.68864300
H	3.46314800	-1.42022200	8.47691000
H	1.73979100	-1.55833700	8.83407900
H	2.64227300	0.64730300	9.50464300
H	3.21560700	0.97445100	7.86139000
H	3.69107500	-3.51633500	7.02979600
H	1.97292100	-3.93508300	7.36795500
H	2.57096600	-3.93248200	5.68864300
H	-3.45622400	1.47680400	-4.46008300
H	-4.45045600	1.06722000	-5.89908900
H	-3.26074800	-0.11336700	-5.20680500
H	4.45045600	-1.06722000	5.89908900
H	3.45622400	-1.47680400	4.46008300
H	3.26074800	0.11336700	5.20680500
H	3.38311500	-2.46650300	-7.25012100
H	-3.38311500	2.46650300	7.25012100
H	-1.86930000	-2.23215500	3.16936600
H	1.86930000	2.23215500	-3.16936600
H	5.94730400	-2.34683600	-3.59808800
H	5.41474200	-0.98019000	-2.65697100
H	-5.41474200	0.98019000	2.65697100
H	-5.94730400	2.34683600	3.59808800
H	4.98299200	1.68780500	2.68518600
H	-4.98299200	-1.68780500	-2.68518600
H	1.38016600	-1.19280900	-3.20343300
H	-1.38016600	1.19280900	3.20343300
H	-1.30600600	-0.13369000	0.76133600
H	-2.98069700	-0.50713300	1.15225600
H	2.98069700	0.50713300	-1.15225600
H	1.30600600	0.13369000	-0.76133600